Optogenetic approaches to characterize the long-range synaptic pathways from the hypothalamus to brain stem autonomic nuclei

Ramón A. Piñol[*], **Ryan Bateman**, and **David Mendelowitz**
Department of Pharmacology and Physiology, The George Washington University, 2300 Eye Street NW, Washington, DC 20037

Abstract

Recent advances in optogenetic methods demonstrate the feasibility of selective photoactivation at the soma of neurons that express channelrhodopsin-2 (ChR2), but a comprehensive evaluation of different methods to selectively evoke transmitter release from distant synapses using optogenetic approaches is needed. Here we compared different lentiviral vectors, with sub-population-specific and strong promoters, and transgenic methods to express and photostimulate ChR2 in the long-range projections of paraventricular nucleus of the hypothalamus (PVN) neurons to brain stem cardiac vagal neurons (CVNs). Using PVN subpopulation-specific promoters for vasopressin and oxytocin, we were able to depolarize the soma of these neurons upon photostimulation, but these promoters were not strong enough to drive sufficient expression for optogenetic stimulation and synaptic release from the distal axons. However, utilizing the synapsin promoter photostimulation of distal PVN axons successfully evoked glutamatergic excitatory post-synaptic currents in CVNs. Employing the Cre/loxP system, using the Sim-1 Cre-driver mouse line, we found that the Rosa-CAG-LSL-ChR2-EYFP Cre-responder mice expressed higher levels of ChR2 than the Rosa-CAG-LSL-ChR2-tdTomato line in the PVN, judged by photo-evoked currents at the soma. However, neither was able to drive sufficient expression to observe and photostimulate the long-range projections to brainstem autonomic regions. We conclude that a viral vector approach with a strong promoter is required for successful optogenetic stimulation of distal axons to evoke transmitter release in pre-autonomic PVN neurons. This approach can be very useful to study important hypothalamus-brainstem connections, and can be easily modified to selectively activate other long-range projections within the brain.

Keywords

Optogenetics; Channelrhodopsin-2; cardiac vagal neuron; paraventricular nucleus of the hypothalamus; cardiovascular; electrophysiology

[*]Corresponding author: Department of Pharmacology and Physiology, The George Washington University, 2300 Eye Street NW, Washington, DC 20037 Tel. +1 202 994 5029, rpinol@gwmail.gwu.edu.

The authors state they have no conflicts of interest.

1. Introduction

Electrical stimulation of neurons and fibers in-vivo within the central nervous system (CNS) has been used for identifying and assessing the targets and responses of long-range synaptic pathways for many years. Although much seminal work has been done with this approach, it possesses several insurmountable inherent obstacles, including limited control over the spread and spatial resolution of stimulation, confounding stimulation of a heterogeneous population of neurons or axons within the stimulated region, unpredictable effectiveness of stimulation that depends on different thresholds for fibers and different neurons within the region, and also the potential for tissue damage. In-vivo studies are also hindered by the inability to apply pharmacological agents in a highly localized area surrounding the target neuron that receives these long –range projections.

In-vitro electrophysiological approaches developed over the last 20 years overcome some of these limitations, such as permitting tight control over the external and internal milieu surrounding cells and allowing more precise stimulation and electrophysiological recordings from neurons. However studies of pathways within in-vitro preparations are limited by the viable depth of the tissue, typically 400–800 microns, and therefore many of the important long-range projections to neurons cannot be studied in-vitro.

A new approach, using optogenetic techniques, overcomes many of these obstacles and potentially enables highly selective stimulation of homogenous neuronal populations, high temporal precision, and activation of synapses originating from neurons distant from the neuron of interest while retaining the high degree of control and precision afforded in-vitro (Fenno et al., 2011). This approach utilizes heterologous expression of the microbial opsin channelrhodopsin-2 (ChR2), a light-activated cation channel that is ubiquitously inserted into the plasma membrane of cells. Brief (millisecond scale) light pulses can depolarize the membrane of cell bodies, dendrites or axons of neurons that express ChR2, allowing for excitation of specific compartments of the plasma membrane, including presynaptic terminals distant from the soma (Petreanu et al., 2007).

Several recent reports have shown the feasibility of this optogenetic method to study the neurophysiology of distant synapses by driving expression of ChR2 using different viral vectors (Cruikshank et al., 2010; Varga et al., 2009) or transgenic mice (Ren et al., 2011). However, a comprehensive comparative assessment of the different available methods has not been done. For instance, it is not readily clear which of the different methods could best drive expression of ChR2 into the plasma membrane of distal synaptic terminals. In order to extend the current knowledge of how to successfully and efficiently employ optogenetic stimulation of distant axons and identified synaptic endings, we tested and compared the usefulness of lentivirus, with neuron- and population-specific promoters, as well as two ChR2 Cre responder transgenic mouse lines to express ChR2 and selectively stimulate the important neurotransmission from paraventricular hypothalamus nucleus (PVN) to brainstem cardiac vagal neurons (CVNs) that control heart rate in the brainstem.

More specifically we tested lentiviral vectors expressing ChR2 under two PVN promoters (minimal promoter regions upstream of the origin of transcription) for vasopressin and oxytocin neurons, and evaluated their ability to drive ChR2 expression in distal axons in autonomic brain stem sites after microinjection in the PVN. We also used a lentiviral vector with a strong neuron-specific promoter (human synapsin I fragment) (Kugler et al., 2003). In addition, we assessed the expression of ChR2 in paraventriculo-autonomic projections using crossbred transgenic mice that express ChR2 in the PVN. To this purpose, we employed the Cre/LoxP system and crossbred two different ChR2 Cre responder lines with a Sim1-Cre driver transgenic mouse. *Sim1* is a gene strongly expressed during embryonic development

in PVN neurons, including in vasopressin and oxytocin parvocellular neurons, that project to the nucleus of the solitary tract (NTS) and dorsal motor nucleus of the vagus (DMV) (Balthasar et al., 2005; Duplan et al., 2009; Fan et al., 1996). In vitro electrophysiology coupled with laser evoked photoactivation of ChR2 was used to assess the functional connectivity of distal autonomic-related PVN projections and to test the effectiveness of each of these approaches in activation of synaptic terminals and transmitter release from PVN neurons onto CVNs.

2. Materials and methods

2.1 Lentiviral vector plasmids and promoter constructs

Lentiviral plasmids pLenti-Syn-hChR2(H134R)-EYFP-WPRE, packaging plasmid pCMV-R8.74 and envelope plasmid pMD2.G were all kindly provided by K. Deisseroth (Stanford University, Stanford, CA). We chose to use the H134R mutant for the current studies for its enhanced photocurrents (Nagel et al., 2005) and higher release probability (Schoenenberger et al., 2011), since our objective was to probe long-range projections and maximize the likelihood of release of neurotransmitter from presynaptic endings. A rat minimal vasopressin promoter fragment containing 527 bp upstream and 30 bp downstream of the start of transcription of the vasopressin gene (UCSC genome browser on rat Nov. 2004 assembly; chr3:118,206,966 to 118,207,522) was de novo synthesized and flanked by multiple cloning sites (Genscript, Piscataway, NJ) (Iwasaki et al., 1997; Kim et al., 2001). Similarly, we synthesized (Genscript, Piscataway, NJ) a rat minimal oxytocin promoter element from −530 bp to +33 relative to the origin of transcription of the oxytocin gene (UCSC genome browser on rat Nov. 2004 assembly; chr3:118,193,690 to 118,194,252) (Chu and Zingg, 1999; Richard and Zingg, 1991). Vasopressin and oxytocin promoter fragments were subcloned into pLenti-Syn-hChR2(H134R)-EYFP-WPRE using the *Xba*I and *Age*I cloning sites to replace the Synapsin promoter, creating the new plasmids pLenti-AVP-hChR2(H134R)-EYFP-WPRE and pLenti-OXY-hChR2(H134R)-EYFP-WPRE.

2.2 Viral vectors

Plasmids pLenti-Syn-hChR2(H134R)-EYFP-WPRE, pLenti-AVP-hChR2(H134R)-EYFP-WPRE and pLenti-OXY-hChR2(H134R)-EYFP-WPRE were transformed into MAX Efficiency Stbl3 Competent Cells for amplification. Plasmids pMD2.G and pCMV-ΔR8.74 were transformed into DH5α cells for amplification and all plasmids were purified using a Maxiprep kit (Qiagen, Valencia, CA). VSVg pseudotyped lentivirus particles were produced according to standard protocols (Szulc et al., 2006). Briefly, we transfected 8–24 1500 mm plates of 60–80% confluent HEK 293T cells with 37.5 μg pLenti, 33 μg pCMV-ΔR8.74 and 18 μg pMD2.G using 2.5 M $CaCl_2$ and 2× HBSS for transfection. Cells were cultured in Dulbecco's modified Eagle's medium (DMEM), 10% FBS (Gibco, Invitrogen), 1% L-glu (Invitrogen) and 1% Pen/Strep (Invitrogen). Eight hours after the transfection, plates were washed with incubation medium and replaced with 13 ml medium. Twenty-four hours after transfection sodium butyrate was added to the plates in a final concentration of 5 mM. The virus was harvested 48 hours after the transfection and the supernatant was spun for 15 minutes at 1500 × g and filtered through a 0.22 μm PES bottle top filter. The supernatant was concentrated by ultracentrifuging for 2 hrs at 20,000 rpm using 38.5 ml thinwall tubes and a Beckmann SW-28 rotor. Viral particles were resuspended in 1–2 ml PBS and pooled for a second 2 hr, 20,000 rpm ultracentrifuge spin into one 10 ml thickwall tube. The final viral vector pellet was resuspended in 35 – 100 μl of PBS, which was stored at − 80° C in 4 μl per aliquot. The viral titer was determined by counting infected HEK 293T cells using FACS (Ramezani and Hawley, 2002). All batches of virus had a titer between 2×10^8 and 1×10^9 transducing units (TU) per ml (see table 1).

2.3 Stereotactic injections, transgenic mice and cardiac labeling

Neonatal Sprague Dawley rats (postnatal day 4 or 5) were anesthetized by hypothermia and mounted in a stereotactic apparatus with a neonatal adapter (Stoelting, Wood Dale, IL). A midline incision exposed the skull and a small burr hole was made to position a pulled calibrated pipette (VWR, Radnor PA) with a thin tip (inner diameter $< 30 \, \mu m$) containing viral vector at the following coordinates: 1.5 – 1.95 mm posterior (depending on the distance between bregma and lambda) and 0.3 mm lateral relative to bregma. The pipette tip was lowered 4.80 mm from the dorsal surface of the brain and 50–350 nl of viral vector was injected at a visually monitored rate of 60 nl per minute. The pipette was left in place for 10 minutes, prior to slow retraction. The incision was closed using surgical glue, antibiotic ointment was applied to closed incisions and animals were warmed up on a heating pad before being returned to their nest. The stereotactic PVN coordinates of postnatal day 5 rat pups were based on (Valenstein et al., 1969) and verified after each experiment for accuracy of the injection sites.

Transgenic mouse Cre-responder lines contain a *loxP*-flanked STOP cassette upstream of the ChR2-tdTomato or ChR2-EYFP fusion gene at the Rosa 26 locus in the following cassettes: Rosa-CAG-LSL-ChR2(H134R)-tdTomato-WPRE-pA (generous gift from H. Zeng, Allen Institute for Brain Science, Seattle, WA; currently available at The Jackson Laboratory, Bar Harbor, ME, stock number 012567) and Rosa-CAG-LSL-ChR2(H134R)-EYFP-WPRE-pA (Stock number 012569, The Jackson Laboratory, Bar Harbor, ME). Cre-responder mice were crossbred with the Cre-driver driver line Sim1-Cre (Stock number 006541, The Jackson Laboratory, Bar Harbor, ME) to obtain ChR2/Sim1 mice that express ChR2 in the PVN.

In order to identify possible target autonomic populations of ChR2 containing PVN axons in the brainstem, we labeled CVNs with a fluorescent tracer (28 rats and 16 mice of both sexes). To label CVNs, the base of the heart in hypothermically anesthetized animals was exposed by a right thoractomy and $20 - 40 \, \mu l$ of X-rhodamine-5-(and 6)-isothiocyanate (XRITC) was injected into the pericardial sac at the base of the heart where cardiac ganglia are located, as described previously (Frank et al., 2009; Kamendi et al., 2006); (Bouairi et al., 2006)The fluorescent tracer XRITC is taken up by axonal endings in the parasympathetic cardiac ganglia and transported retrogradely to the cell bodies of CVNs in the DMV and NA. All efforts were made to minimize the number of animals used and to avoid any possible discomfort. All animal procedures were performed in compliance with the institutional guidelines at The George Washington University and are in accordance with the recommendations of the Panel on Euthanasia of the American Veterinary Medical Association and the National Institutes of Health publication Guide for the Care and Use of Laboratory Animals.

2.4 Slice preparation and electrophysiology

For brain stem slice electrophysiology rats and mice between P21 and P80 were anesthetized and sacrificed, and transcardially perfused and exsanguinated with ice-cold glycerol-based aCSF (252 mM glycerol, 1.6 mM KCl, 1.2 mM NaH_2PO_4, 1.2 mM $MgCl_2$, 1.2 mM $CaCl_2$, 18 mM $NaHCO_3$, 11 mM glucose, 1.0 mM pyruvic acid and 1.0 mM ascorbic acid, perfused with 95% O_2 and 5% CO_2, pH = 7.4). For younger animals the transcardiac perfusion was omitted. The brain was carefully removed and brainstem slices ($300 \, \mu m$) were obtained using a vibratome (all in the glycerol-based aCSF), as well as forebrain slices ($100 \, \mu m$ for immunohistochemistry, $160 \, \mu m$ for injection site verification and $250 \, \mu m$ for electrophysiology) containing the PVN. Slices were allowed to recover at 32 °C in aCSF (125 mM NaCl, 3 mM KCl, 2 mM CaCl2, 26 mM $NaHCO_3$, 5 mM glucose, and 5 mM HEPES, perfused with 95% O_2 and 5% CO_2, pH = 7.4) for 30 minutes, before being

mounted in a perfusion chamber and submerged in 22–24 ℃ room temperature aCSF perfusate. Experiments were performed on a Nikon Eclipse E600FN using a 40× water immersion objective. Identified CVNs were imaged with differential interference contrast optics, infrared illumination, and infrared-sensitive video detection cameras to gain better spatial resolution. A 473 nm blue CrystaLaser (Reno, NV), attached to the microscope using a dual housing adapter (Nikon) was used for photostimulation of ChR2 with short light pulses of 1 – 3 ms at indicated frequencies. The numerical aperture of the 40X water immersion objective was 0.8 and the working distance 2.0 mm. Stimulations were performed at indicated frequencies. For 1 and 2 Hz frequencies a minimum of 25 sweeps were used for analysis. Laser light intensity was kept constant across all experiments at an output of 10 mW, an empirically defined intensity beyond which ChR2 responses (both at soma and post-synaptical) did not increase. Patch pipettes (2.5–4.5 MOhm) contained 135 mM K gluconic acid, 10 mM HEPES, 10 mM EGTA, 1mM $CaCl_2$, 1 mM $MgCl_2$ and 2 mM Na-ATP, pH = 7.3, or, before having established that the response was excitatory, 150 mM KCl, 4 mM $MgCl_2$, 2 mM EGTA, 2 mM Na-ATP and 10 mM HEPES, pH 7.4. Synaptic activity from the identified CVN was recorded at −80mV. Voltage-clamp and current-clamp whole-cell recordings were made with an Axopatch 200B and pClamp 9 software (Axon Instruments, Union City, CA, USA). Synaptic events and peak amplitudes were detected using Clampfit 10.1. Jitter and average onset latency (standard deviation of the average onset latency) was analyzed by determining >30 photo-activated synaptic events in each cell (Bailey et al., 2006).

The following drugs were diluted from a stock solution and applied to the perfusate: strychnine (1 µM), gabazine (25 µM), tetrodotoxin (TTX; 1 µM) D-2-amino-5-phosphonovalerate (AP-5; 50 µM), and 6-cyano-7-nitroquinoxaline-2,3-dione (CNQX; 50 µM)

2.5 Immunohistochemistry and imaging

Slices processed for immunohistochemistry, ChR2-expressing cell bodies in the PVN, and axons and synaptic terminals in the brain stem were visualized after the electrophysiological experiments upon placing the brainstem and hypothalamic tissue in 10% formalin, and the tissue was mounted and cover slipped with Prolong anti-fade mounting medium (Invitrogen, Eugene, OR). In PVN-containing slices the injection site was examined to assess whether the viral vector had spread to adjacent brain regions. If the viral vector injection spread outside of the PVN the experiments from this animal were discarded.

To determine the specificity of the OXY-ChR2-EYFP and AVP-ChR2-EYFP promoters immunohistochemistry was utilized to co-localize oxytocin, vasopressin and viral expression of EYFP. Slices were soaked overnight in 10% formalin and were processed for oxytocin-, vasopressin- and EYFP using the following primary antibodies (overnight incubation at 22–24 ℃): guinea pig anti-AVP antibody (1:15000 dilution; T-5048, Bachem, Torrance, CA), rabbit anti-oxytocin antibody (1:15000 dilution; T-4084, Bachem, Torrance, CA) and mouse anti-GFP/EYFP (1:500 dilution; ab38689, Abcam, Cambridge, MA). As secondary antibodies we used goat anti-guinea pig Alexa Fluor 633, goat anti rabbit Alexa Fluor 405 and chicken anti-mouse Alexa Fluor 488 (all 1:200 dilution and 4 h incubation at 22–24 ℃; Life Technologies, Carlsbad, CA).

Low magnification pictures were generated using an inverted Motic AE31 microscope. PVN and brainstem slices were used for confocal microscopy. Stack images (12 – 80 µm; collapsed into 2D images) and tile scans were collected with the 20x and 63x objective of the Zeiss 710 confocal system and composed with Volocity software. For colocalization analysis, slice we used a 60 µm z-stack image of every other 100 µm for offline analysis. ChR2-EYFP cells were counted and examined for positive colocalization with oxytocin and

vasopressin at three different levels of the PVN along the rostro-caudal axis (Bregma −1.5, −1.7 and −1.9).

3. Results

3.1 PVN subpopulation-specific lentiviral vectors: OXY-ChR2-EYFP and AVP-ChR2-EYFP

3.1.1 PVN Injection site—To examine long-range and selective PVN projections to caudal brain stem sites two PVN-specific lentiviral vectors, one driving ChR2-EYFP expression by an oxytocin promoter and another using a vasopressin promoter, were tested. Both viral vectors successfully infected PVN neurons, with very few to no infected cell bodies outside the boundaries of the PVN. Immunohistochemical analysis confirmed that a very large fraction (93 ± 2.0 %) of neurons infected with OXY-ChR2-EYP stained positive for oxytocin (see fig 1a–d). None of the OXY-ChR2-EYFP cells stained positive for vasopressin. In animals injected with the AVP-ChR2-EYFP virus there was no expression in OXY neurons. In these animals expression was detected in both AVP neurons and unidentified PVN neurons. While the AVP promoter was selective for non-OXY neurons, the AVP-ChR2-EYFP virus labeled neurons that included both AVP and a majority of non-AVP/non-OXY neurons (data not shown).

To examine the ChR2 evoked currents in the soma of PVN neurons using these viral vectors ChR2-EYFP labeled PVN neurons in the dorsal and medial parvocellular subdivisions of the PVN were studied using patch clamp techniques 25–30 days after virus injection into the PVN. Photoactivated currents were recorded in the presence of AP-5 and CNQX to block glutamatergic neurotransmission and TTX to block action potential generation. Photoexcitation, at a frequency of 1 Hz, yielded large currents, 221.1 ± 66.0 pA (n = 7) and 86.3 ± 31.5 pA (n= 8) in OXY-ChR2-EYFP (Fig. 2a) and AVP-ChR2-EYFP (Fig. 2d) rats, respectively. The larger amplitude of currents upon stimulation of the cell bodies in OXY-ChR2-EYFP animals suggests that the OXY-ChR2-YFP drives stronger expression than AVP-ChR2-EYFP, since other work has shown the generated current is proportional to the expression level of ChR2 (Schoenenberger et al., 2011). This indicates a poor expression of ChR2 using the AVP promoter despite the higher titer of the AVP-ChR2-EYFP virus compared to the OXY-ChR2-EYFP virus. Nevertheless, with both viruses optogenetically induced currents were large enough to generate single action potentials (Fig. 2b, 2c) and action potential trains in PVN neurons when stimulated at a frequency of 10Hz (Fig. 2e).

3.1.2 ChR2-EYFP axons in brainstem—To test whether these promoters are strong enough to drive ChR2-EYFP expression sufficient to photoactive distal axons and synaptic terminals, we examined the distant projections of these hypothalamic neurons in the brainstem. Axons in the caudal brainstem were not observed until 35 days after injection of OXY-ChR2-EYFP. We observed a low number of axons in the NTS and DMV (Fig. 1e), none in the Amb and very few at the ventral medullary surface. In contrast, there was an absence of AVP-ChR2-EYFP labeled axons, even 75 days post virus injection. Neither of these promoters expressed ChR2 sufficiently to photoexcite axons or synaptic terminals and evoke transmitter release onto CVNs between 35 and 75 days after the injection.

3.2 ChR2 expression in PVN with a neuron-specific lentiviral vector: Syn-ChR2-EYFP

3.2.1 PVN Injection site—Since photostimulation of distal axons of PVN neurons did not successfully evoke transmitter release and postsynaptic currents upon utilizing viral vectors that drive ChR2 in a genetically defined subpopulation using oxytocin or vasopressin promoters, we opted to use a promoter that might yield a higher expression of ChR2 in the presynaptic terminals. A lentiviral vector that drives ChR2-EYFP expression by a synapsin

promoter fragment was injected into the PVN (Fig. 3a). Animals with injection sites that contained infected neurons outside the PVN were excluded from further analysis.

Functional expression was tested by photostimulating fluorescently-identified PVN neurons in pre-autonomic PVN subdivisions. Peak currents were recorded in the presence of AP-5, CNQX and TTX. Activation of ChR2 in the soma of these PVN neurons yielded large currents of 268 ± 42.8 pA (n = 7) when stimulating at 1 Hz (Fig. 3b). This ChR2 evoked current reliably elicited action potentials (1Hz stimulation) in these PVN neurons (Fig. 3c).

3.2.2 ChR2-EYFP axons in brainstem—ChR2-EYFP axonal projections were detected in the brainstem from 20 days post injection and EYFP fluorescent intensity continued to increase until ~ 40 days post viral microinjection. Fluorescent axons and terminals were consistently observed in the rostral medulla (Fig. 3d–f), more specifically in the NTS, DMV, Amb, ventrolateral medulla, including A1/C1 and ventral respiratory groups, ventral medullary surface and in the reticular formation between Amb and NTS. This pattern of PVN-originating fibers corresponds very closely with prior neuroanatomical studies that indicate functional connectivity between the PVN and medullary sites involved in autonomic control (Geerling et al., 2010; Saper et al., 1976; Sawchenko and Swanson, 1982). The highest density of axons was observed in the NTS and the ventral medullary surface, followed by the expression of fibers in the DMV. A moderately high density of axons was observed in the Amb. PVN ChR2-EYP axons and putative boutons were found in close apposition to preganglionic cardiac vagal neurons in this area (Fig. 3e, 3f), as well as in the DMV (not shown).

In order to study the synaptic activation of long-range paraventriculo-autonomic projections to the brainstem we photoexcited ChR2-EYFP axons in the caudal medullary slices containing Amb and DMV 25 days after injection of the virus into the PVN. Brief light pulses (1–3 ms) generated large post-synaptic responses in whole-cell voltage-clamped CVNs in DMV (Fig. 3g). The short latency time (average: 5.44 ms $\pm$ 0.39, n=11, ranging from 3.8 – 7.8 ms) suggests that there is likely a direct monosynaptic pathway from hypothalamic PVN neurons to brainstem CVNs. We observed an average failure rate of 4.5 % $\pm$ 2.06 (n=7, ranging from 0 to 15.6 %). Typical average latencies for monosynaptic transmission using optogenetic stimulation of axons in other studies range between 3.6 and 17.3 ms and polysynaptic latencies typically vary between 18 and 25.6 ms (Petreanu et al., 2007; Petreanu et al., 2009; Ren et al., 2011; Toni et al., 2008; Wang et al., 2009; Xiong et al., 2012). In support of a monosynaptic connection, the low jitter (0.83 $\pm$ 0.09 ms, n=7) of the synaptic responses in this study fall in the reported range for monosynaptic pathways (Petreanu et al., 2007; Petreanu et al., 2009; Xiong et al., 2012). To further characterize the nature of this neurotransmission, we applied antagonists selective for ionotropic GABA(A) and glycine receptors (gabazine and strychnine, respectively). Neither gabazine nor strychnine caused any significant change in the amplitude or kinetics of the light-evoked post-synaptic currents in CVNs in the DMV (Fig. 2h, red trace). However application of the AMPA/kainate and NMDA receptor selective antagonists, CNQX (50 μM) and AP-5 (50 μM), respectively, abolished the synaptic neurotransmission. In addition, we tested whether optogenetic stimulation of ChR2- containing axon terminals can be used to obtain a measure of synaptic function, such as paired pulse ratio (PPR). PPR is frequently used to asses short-term plasticity, and can assess fundamental differences in presynaptic release of neurotransmitter and postsynaptic sensitivity between two experimental groups of animals (Citri and Malenka, 2008; Kline et al., 2007). We found paired-pulse facilitation in the PVN to CVN neurotransmission (Fig. 3i), as expressed using paired-pulse ratio (PPR = response 2/response 1). PPR facilitation at 10 Hz was 1.62 $\pm$ 0.22 (n= 6).

3.3 Transgenic mice expressing ChR2 in PVN

The viral vectors with PVN-specific promoters were not able to yield optogenetic mediated transmitter release and post-synaptic currents in the DMV and Amb, and while lentivirus mediated expression of the PVN terminals can successfully evoke transmitter release and generate postsynaptic responses, this approach requires a high degree of specificity in injection to insure selective infection of neurons solely within the PVN. We therefore additionally explored a Cre/loxP transgenic mice approach to use the advantages of genetic targeting. Upon crossbreeding of Sim1-Cre and ChR2-tdTomato reporter mice we detected expression of the ChR2-tdTomato fusion protein in PVN neurons of ChR2-tdTomato/Sim1 mice at early postnatal ages (Fig. 4a, c). Functional ChR2 expression in PVN neurons was confirmed in ChR2-tdTomato/Sim1 mice at P6 and P13, in which 3 ms light exposures yielded average currents of 11.2 ± 0.9 pA (n=5) and 7.5 ± 1.2 pA (n=5), respectively (Fig 4b). However, these currents were small and were nearly always insufficient to evoke action potentials in the PVN neurons. In caudal brain stem slices, we were unable to observe any ChR2-tdTomato in young animals (P4 – P18, n = 12) or at older ages (P44 – P56, n=6). In accordance with the absence of visually detectable ChR2 axons in brain stem slices, we were unable to discern any optogenetically generated post-synaptic currents in neurons in the DMV in ChR2-tdTomato/Sim1 mice. The combination of small light-evoked ChR2 currents in PVN neurons and no discernable ChR2 axons or currents in the brainstem suggests insufficient levels of ChR2 expression required for optogenetic stimulation of this pathway.

In addition, we tested whether another ChR2 Cre-responder line was able to drive higher levels of expression. We generated the ChR2-EYFP/Sim1 crossbreed and observed functional ChR2-EYFP expression in young animals. Optogenetic stimulation resulted in a response of 48.4 ± 12.0 pA (n=7) at P9–10 (Fig. 4d). When stimulated at a frequency of 0.05 Hz, cells with a larger response could drive action potential generation (Fig. 4e). Larger responses in PVN neurons indicate higher expression levels of ChR2 in the ChR2-EYFP mouse compared to the ChR2-tdTomato mouse, however, we did not observe any fibers, nor could we evoke any transmitter release in the brainstem of P35 – P65 ChR2-EYFP/Sim1 mice.

4. Discussion

The results of this study demonstrate that a VSVg pseudotyped lentiviral vector with a strong neuronal promoter (human synapsin1 fragment) is able to drive ChR2-EYFP expression in PVN neurons sufficient to optogenetically stimulate the distal pre-autonomic synaptic endings and evoke transmitter release onto CVNs located in the brainstem. Testing lentiviral vectors with PVN specific promoters (minimal upstream promoter regions of AVP and oxytocin genes), we found a very low number of ChR2-EYFP-positive fibers in the dorsal vagal complex in the brainstem of OXY-ChR2-EYFP animals, but no fibers were observed in AVP-ChR2-EYFP rats. Correspondingly, we were not able to elicit EPSCs in CVNs upon photostimulation of PVN axons in the brainstem using either of these vectors. Using a transgenic mouse approach that genetically targeted pre-autonomic PVN neurons by crossbreeding Sim1-Cre mice with ChR2-Cre responder mouse lines, our results indicate that the Rosa-CAG-LSL-ChR2-EYFP line expresses higher levels of ChR2 in the PVN than the Rosa-CAG-LSL-ChR2-tdTomato line. Nevertheless, we were unable to find EYFP expression of ChR-EYFP in PVN axons or optogenetically evoke EPSCs in the brain stem of Sim1-Cre/ChR2-EYFP animals.

Although the lentiviral vector OXY-ChR2-EYFP was able to express ChR2 in some fibers in the brainstem, we could not optogenetically induce EPSCs in CVNs using this approach. This finding was surprising since oxytocin has been shown to modulate the vagal afferent input in nearby NTS neurons (Peters et al., 2008) and more importantly it has been reported

that oxytocin excites virtually all DMV neurons in the rat (Raggenbass et al., 1987). These results suggest there is not enough ChR2 expression using this approach to generate action potentials at the presynaptic terminal and release neurotransmitter. It is likely that a substantial number of ChR2 molecules are required for depolarization of an axon and subsequent presynaptic vesicle release, and the expression levels of ChR2 using the OXY and AVP viruses are insufficient.

Several studies have used viral vectors with population specific promoters (Abbott et al., 2009; Adamantidis et al., 2007; Knobloch et al., 2012) to optogenetically target a subpopulation and excite these neurons at their soma. Of these studies, only Knobloch and colleagues (2012) examined photoexcitation of distal axons. The study by Knobloch and colleagues used a 2.6 kb mouse OXY promoter to drive ChR2 expression and demonstrated optogenetic activation of PVN oxytocinergic terminals in the amygdala. While similar in many ways to this study, there are some important differences. Knobloch et al. concluded that the fibers that they stimulate are from the neurosecretory magnocellular population of neurons of the PVN and that the endings of the PVN neurons that they stimulate in the CeA have collaterals to the pituitary. In contrast, the PVN population that was examined in this study are neurons in the parvocellular non-secretory PVN population that rather has important descending projections to the brainstem and spinal cord. Whereas Knobloch et al. used only lactating rats which likely enhances ChR2 expression for this limited period as lactating rats produce more oxytocin, (and raises the issue of whether the approach used by Knobloch is limited to lactating animals and might not be effective in male or non-lactating females) our results describe successful approaches that can be used in animals of both sexes without requiring heightened behaviorally mediated expression.

A possible solution to the lower expression levels of OXY-ChR2-EYFP and AVP-ChR2-EYFP observed in this study could be the use of two viral vectors in combination with the Cre/lox system. In this approach, one viral vector expresses Cre under a specific promoter (for instance, a specific oxytocin or AVP promoter fragment) and the other is a Cre-dependent vector expressing ChR2 under a strong promoter. This approach of combining two viruses has been shown to be successful in optogenetically stimulating fibers of piriform cortex neurons almost 2 mm away from the injection site of the viral vectors (Franks et al., 2011).

Our transgenic mouse approach failed to drive adequate levels of expression to have ChR2 inserted in the membrane of long-range projections. Channelrhodopsin-2 expression levels in Sim1/ChR2-EYFP however appeared higher than in Sim1/ChR2-td-Tomato mice, as judged by the photoactivated current generated at the cell body. It is unknown whether this variation is contributable to inter-strain differences or to differences between protein transfer kinetics of td-Tomato and EYFP. Compared to the lentiviral approach, the transgenic mice would presumably have less copies of the ChR2 gene, since it is likely that high titer lentiviral vectors integrate multiple copies of the gene. This would be consistent with our results of limited expression using the transgenic mouse compared to the lentivirus driven expression. Possible approaches to overcome this limited expression could include the use of different promoters as other stronger promoters (such as synapsin, CaMKII, Ef1a) might drive higher levels of expression in PVN neurons. Another approach to overcome this problem could be to tag the ChR2-XFP with a domain that directs the insertion of ChR2 to the presynaptic terminal. This approach has been used to localize ChR2 to the axon initial segment (Grubb and Burrone, 2010) and the somatodendritic compartment (Lewis et al., 2009).

In contrast to our system, a recent study using a BAC transgenic approach to express ChR2-EYFP in distal axons of habenular ChAT neurons allows for optogenetic stimulation of

distal axons in the interpeduncular nucleus (Ren et al., 2011). Another study using the BAC approach reporting several cell type-specific ChR2 mice also observed light-evoked neurotransmitter release from distal axons (Zhao et al., 2011). In addition, in Mrgprd-ChR2-venus mice that express ChR2 in dorsal root ganglia nociceptive neurons, ChR2 fibers were detected in the skin (Wang and Zylka, 2009). In these three studies mice were of a similar age as the Sim1/ChR2 mice that we assessed. Interestingly, it is noteworthy that in our Sim1/ChR2 animals another long-range projection from Sim-1 neurons in the mammillary body to the anterior thalamic nucleus (mammillo-thalamic tract) expresses a high level of ChR2, as judged by the dense network of labeled fibers (data not shown), suggesting there may be a high variability of expression in different pathways within the same animal model.

Previous work has shown stimulation of the PVN elicits a bradycardia (Darlington et al., 1989), however the pathways and mechanisms underlying these responses were previously unknown. The results in this study establish a likely monosynaptic pathway from the PVN to parasympathetic cardiac vagal neurons that project to the heart. Furthermore, this pathway is excitatory, uses glutamate as a primary transmitter, and exhibits paired pulse facilitation. The approaches evaluated in this study will allow a more detailed characterization of this and other distant pathways in the CNS, which was not possible prior to the use of optogenetic advances in neuroscience research.

Acknowledgments

Abbreviations

12	Hypoglossal Nucleus
3V	Third Ventricle
Amb	Nucleus Ambiguus
AP-5	D-2-amino-5-phosphonovalerate
AVP	Arginine vasopressin
cc	Central Canal
ChR-2	Channelrhodpsin-2
CNS	Central Nervous systems
CNQX	6-cyano-7-nitroquinoxaline-2,3-dione
CVN	Cardiac vagal Neuron
DMV	Dorsal Motor Nucleus of the Vagus
GABA	Gamma-Aminobutyric Acid
NTS	Nucleus of the Solitary Tract
OXY	Oxytocin
PPR	Paired-pulse response
PVN	Paraventricular Nucleus of the Hypothalamus

Sim1	Single-minded homolog 1
SON	Supraoptic Nucleus
TTX	Tetrodotoxin
XRITC	X-rhodamine-5-(and 6)-isothiocyanate

References

Abbott SB, Stornetta RL, Fortuna MG, Depuy SD, West GH, Harris TE, Guyenet PG. Photostimulation of retrotrapezoid nucleus phox2b-expressing neurons in vivo produces long-lasting activation of breathing in rats. J Neurosci. 2009; 29:5806–19. [PubMed: 19420248]

Adamantidis AR, Zhang F, Aravanis AM, Deisseroth K, de Lecea L. Neural substrates of awakening probed with optogenetic control of hypocretin neurons. Nature. 2007; 450:420–4. [PubMed: 17943086]

Bailey TW, Jin YH, Doyle MW, Smith SM, Andresen MC. Vasopressin inhibits glutamate release via two distinct modes in the brainstem. J Neurosci. 2006; 26:6131–42. [PubMed: 16763021]

Balthasar N, Dalgaard LT, Lee CE, Yu J, Funahashi H, Williams T, Ferreira M, Tang V, McGovern RA, Kenny CD, Christiansen LM, Edelstein E, Choi B, Boss O, Aschkenasi C, Zhang CY, Mountjoy K, Kishi T, Elmquist JK, Lowell BB. Divergence of melanocortin pathways in the control of food intake and energy expenditure. Cell. 2005; 123:493–505. [PubMed: 16269339]

Bouairi E, Kamendi H, Wang X, Gorini C, Mendelowitz D. Multiple types of GABAA receptors mediate inhibition in brain stem parasympathetic cardiac neurons in the nucleus ambiguus. J Neurophysiol. 2006; 96:3266–72. [PubMed: 16914614]

Chu K, Zingg HH. Activation of the mouse oxytocin promoter by the orphan receptor RORalpha. J Mol Endocrinol. 1999; 23:337–46. [PubMed: 10601979]

Citri A, Malenka RC. Synaptic plasticity: multiple forms, functions, and mechanisms. Neuropsychopharmacology. 2008; 33:18–41. [PubMed: 17728696]

Cruikshank SJ, Urabe H, Nurmikko AV, Connors BW. Pathway-specific feedforward circuits between thalamus and neocortex revealed by selective optical stimulation of axons. Neuron. 2010; 65:230–45. [PubMed: 20152129]

Darlington DN, Miyamoto M, Keil LC, Dallman MF. Paraventricular stimulation with glutamate elicits bradycardia and pituitary responses. Am J Physiol. 1989; 256:R112–9. [PubMed: 2563205]

Duplan SM, Boucher F, Alexandrov L, Michaud JL. Impact of Sim1 gene dosage on the development of the paraventricular and supraoptic nuclei of the hypothalamus. Eur J Neurosci. 2009; 30:2239–49. [PubMed: 20092567]

Fan CM, Kuwana E, Bulfone A, Fletcher CF, Copeland NG, Jenkins NA, Crews S, Martinez S, Puelles L, Rubenstein JL, Tessier-Lavigne M. Expression patterns of two murine homologs of Drosophila single-minded suggest possible roles in embryonic patterning and in the pathogenesis of Down syndrome. Mol Cell Neurosci. 1996; 7:1–16. [PubMed: 8812055]

Fenno L, Yizhar O, Deisseroth K. The development and application of optogenetics. Annu Rev Neurosci. 2011; 34:389–412. [PubMed: 21692661]

Frank JG, Jameson HS, Gorini C, Mendelowitz D. Mapping and identification of GABAergic neurons in transgenic mice projecting to cardiac vagal neurons in the nucleus ambiguus using photo-uncaging. J Neurophysiol. 2009; 101:1755–60. [PubMed: 19164103]

Franks KM, Russo MJ, Sosulski DL, Mulligan AA, Siegelbaum SA, Axel R. Recurrent circuitry dynamically shapes the activation of piriform cortex. Neuron. 2011; 72:49–56. [PubMed: 21982368]

Geerling JC, Shin JW, Chimenti PC, Loewy AD. Paraventricular hypothalamic nucleus: axonal projections to the brainstem. J Comp Neurol. 2010; 518:1460–99. [PubMed: 20187136]

Grubb MS, Burrone J. Channelrhodopsin-2 localised to the axon initial segment. PLoS One. 2010; 5:e13761. [PubMed: 21048938]

Iwasaki Y, Oiso Y, Saito H, Majzoub JA. Positive and negative regulation of the rat vasopressin gene promoter. Endocrinology. 1997; 138:5266–74. [PubMed: 9389510]

Kamendi H, Dergacheva O, Wang X, Huang ZG, Bouairi E, Gorini C, Mendelowitz D. NO differentially regulates neurotransmission to premotor cardiac vagal neurons in the nucleus ambiguus. Hypertension. 2006; 48:1137–42. [PubMed: 17015774]

Kim JK, Summer SN, Wood WM, Schrier RW. Role of glucocorticoid hormones in arginine vasopressin gene regulation. Biochem Biophys Res Commun. 2001; 289:1252–6. [PubMed: 11741329]

Kline DD, Ramirez-Navarro A, Kunze DL. Adaptive depression in synaptic transmission in the nucleus of the solitary tract after in vivo chronic intermittent hypoxia: evidence for homeostatic plasticity. J Neurosci. 2007; 27:4663–73. [PubMed: 17460079]

Knobloch HS, Charlet A, Hoffmann LC, Eliava M, Khrulev S, Cetin AH, Osten P, Schwarz MK, Seeburg PH, Stoop R, Grinevich V. Evoked axonal oxytocin release in the central amygdala attenuates fear response. Neuron. 2012; 73:553–66. [PubMed: 22325206]

Kugler S, Kilic E, Bahr M. Human synapsin 1 gene promoter confers highly neuron-specific long-term transgene expression from an adenoviral vector in the adult rat brain depending on the transduced area. Gene therapy. 2003; 10:337–47. [PubMed: 12595892]

Lewis TL Jr, Mao T, Svoboda K, Arnold DB. Myosin-dependent targeting of transmembrane proteins to neuronal dendrites. Nat Neurosci. 2009; 12:568–76. [PubMed: 19377470]

Nagel G, Brauner M, Liewald JF, Adeishvili N, Bamberg E, Gottschalk A. Light activation of channelrhodopsin-2 in excitable cells of Caenorhabditis elegans triggers rapid behavioral responses. Current biology: CB. 2005; 15:2279–84. [PubMed: 16360690]

Paxinos, G.; Watson, C. The rat brain in stereotaxic coordinates. 6. Elsevier Academic Press; San Diego, CA: 2007.

Peters JH, McDougall SJ, Kellett DO, Jordan D, Llewellyn-Smith IJ, Andresen MC. Oxytocin enhances cranial visceral afferent synaptic transmission to the solitary tract nucleus. J Neurosci. 2008; 28:11731–40. [PubMed: 18987209]

Petreanu L, Huber D, Sobczyk A, Svoboda K. Channelrhodopsin-2-assisted circuit mapping of long-range callosal projections. Nat Neurosci. 2007; 10:663–8. [PubMed: 17435752]

Petreanu L, Mao T, Sternson SM, Svoboda K. The subcellular organization of neocortical excitatory connections. Nature. 2009; 457:1142–5. [PubMed: 19151697]

Raggenbass M, Dubois-Dauphin M, Charpak S, Dreifuss JJ. Neurons in the dorsal motor nucleus of the vagus nerve are excited by oxytocin in the rat but not in the guinea pig. Proc Natl Acad Sci U S A. 1987; 84:3926–30. [PubMed: 3473490]

Ramezani, A.; Hawley, RG. Generation of HIV-1-based lentiviral vector particles. In: Ausubel, Frederick M., et al., editors. Current protocols in molecular biology. Vol. Chapter 16. 2002. p. 22

Ren J, Qin C, Hu F, Tan J, Qiu L, Zhao S, Feng G, Luo M. Habenula "cholinergic" neurons co-release glutamate and acetylcholine and activate postsynaptic neurons via distinct transmission modes. Neuron. 2011; 69:445–52. [PubMed: 21315256]

Richard S, Zingg HH. Identification of cis-acting regulatory elements in the human oxytocin gene promoter. Mol Cell Neurosci. 1991; 2:501–10. [PubMed: 19912835]

Saper CB, Loewy AD, Swanson LW, Cowan WM. Direct hypothalamo-autonomic connections. Brain Res. 1976; 117:305–12. [PubMed: 62600]

Sawchenko PE, Swanson LW. Immunohistochemical identification of neurons in the paraventricular nucleus of the hypothalamus that project to the medulla or to the spinal cord in the rat. J Comp Neurol. 1982; 205:260–72. [PubMed: 6122696]

Schoenenberger P, Scharer YP, Oertner TG. Channelrhodopsin as a tool to investigate synaptic transmission and plasticity. Exp Physiol. 2011; 96:34–9. [PubMed: 20562296]

Szulc J, Wiznerowicz M, Sauvain MO, Trono D, Aebischer P. A versatile tool for conditional gene expression and knockdown. Nat Methods. 2006; 3:109–16. [PubMed: 16432520]

Toni N, Laplagne DA, Zhao C, Lombardi G, Ribak CE, Gage FH, Schinder AF. Neurons born in the adult dentate gyrus form functional synapses with target cells. Nat Neurosci. 2008; 11:901–7. [PubMed: 18622400]

Valenstein T, Case B, Valenstein ES. Stereotaxic atlas of the infant rat hypothalamus. Developmental psychobiology. 1969; 2:75–80. [PubMed: 4949806]

Varga V, Losonczy A, Zemelman BV, Borhegyi Z, Nyiri G, Domonkos A, Hangya B, Holderith N, Magee JC, Freund TF. Fast synaptic subcortical control of hippocampal circuits. Science. 2009; 326:449–53. [PubMed: 19833972]

Wang H, Zylka MJ. Mrgprd-expressing polymodal nociceptive neurons innervate most known classes of substantia gelatinosa neurons. J Neurosci. 2009; 29:13202–9. [PubMed: 19846708]

Wang J, Hasan MT, Seung HS. Laser-evoked synaptic transmission in cultured hippocampal neurons expressing channelrhodopsin-2 delivered by adeno-associated virus. J Neurosci Methods. 2009; 183:165–75. [PubMed: 19560489]

Xiong Q, Oviedo HV, Trotman LC, Zador AM. PTEN regulation of local and long-range connections in mouse auditory cortex. J Neurosci. 2012; 32:1643–52. [PubMed: 22302806]

Zhao S, Ting JT, Atallah HE, Qiu L, Tan J, Gloss B, Augustine GJ, Deisseroth K, Luo M, Graybiel AM, Feng G. Cell type-specific channelrhodopsin-2 transgenic mice for optogenetic dissection of neural circuitry function. Nat Methods. 2011; 8:745–52. [PubMed: 21985008]

Highlights

- Lentiviral vectors were injected into PVN to express ChR2-EYFP under oxytocin, vasopressin or synapsin promoter

- Only synapsin promoter was strong enough to optogenetically stimulate long-range axon endings in brainstem autonomic nuclei

- All three promoters could generate action potential firing at PVN cell bodies

- Crossbreeding ChR2 Cre with Sim1-Cre mice allowed optogenetic PVN neuron stimulation, but not at brain stem distal axons

- Useful approach to study important hypothalamus-brainstem connections; easily modifiable for other long-range projections.
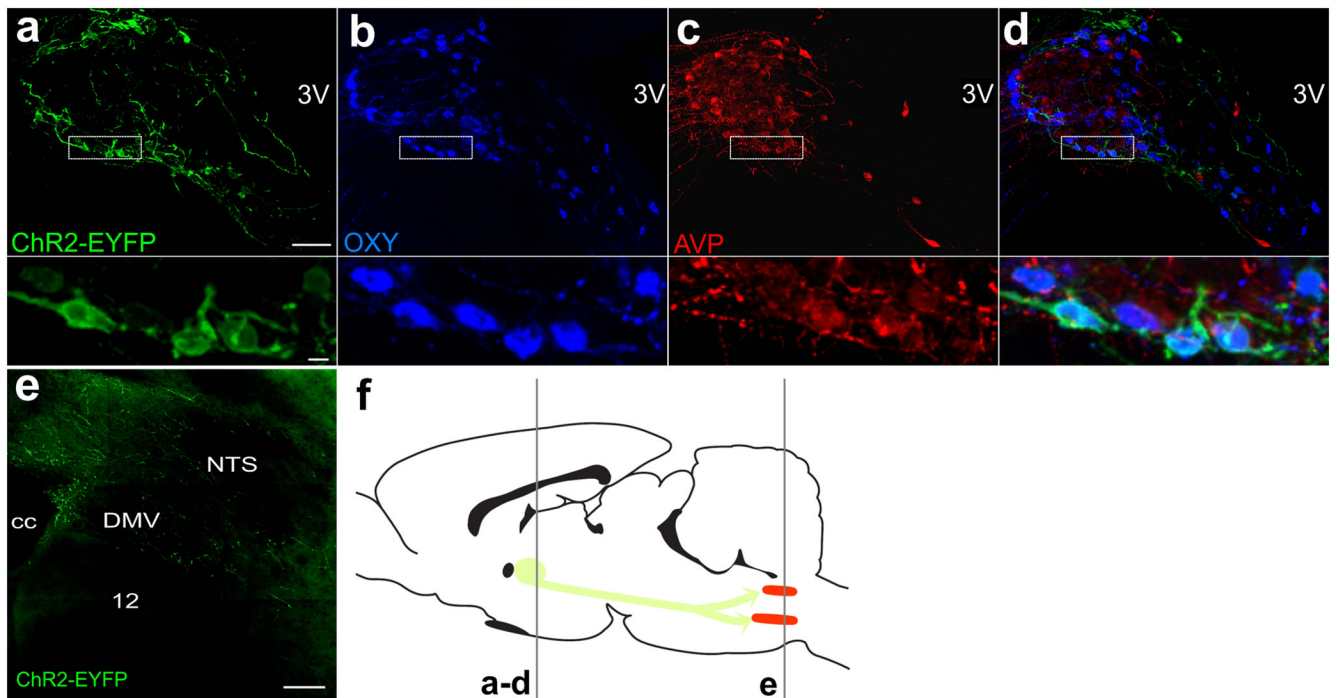
Fig. 1.

Subpopulation-specific lentiviral vector OXY-ChR2-EYFP expresses ChR2-EYFP in PVN neurons and in distal axons in the brain stem. Confocal images of immunohistochemical staining of the PVN of an animal injected with the OXY-ChR2-YFP lentiviral vector for ChR2-EYFP (a), oxytocin (b), vasopressin (c) and the merged image (d), each with a panel underneath with higher magnification. Scale bar is 90 μm for the top images, and 10 μm for the more detailed panels below (a–d). (e) Distal axons of PVN neurons infected with OXY-ChR2-EYFP in the dorsal vagal complex in the brainstem (scale bar represents 150 μm). (f) Schematic depiction of rat brain in sagital orientation, indicating rostro-caudal levels at which slices are taken. Slices containing the PVN (green) are taken at the level of the rostral gray line and brain stem slices containing CVNs in the DMV and Amb (both nuclei represented in red) at the caudal gray line. Schematic picture was adapted from Paxinos and Watson (2007). Hypoglossal Nucleus; 3V, Third Ventricle; cc, Central Canal; DMV, Dorsal Motor Nucleus of the Vagus; NTS, Nucleus of the Solitary Tract.
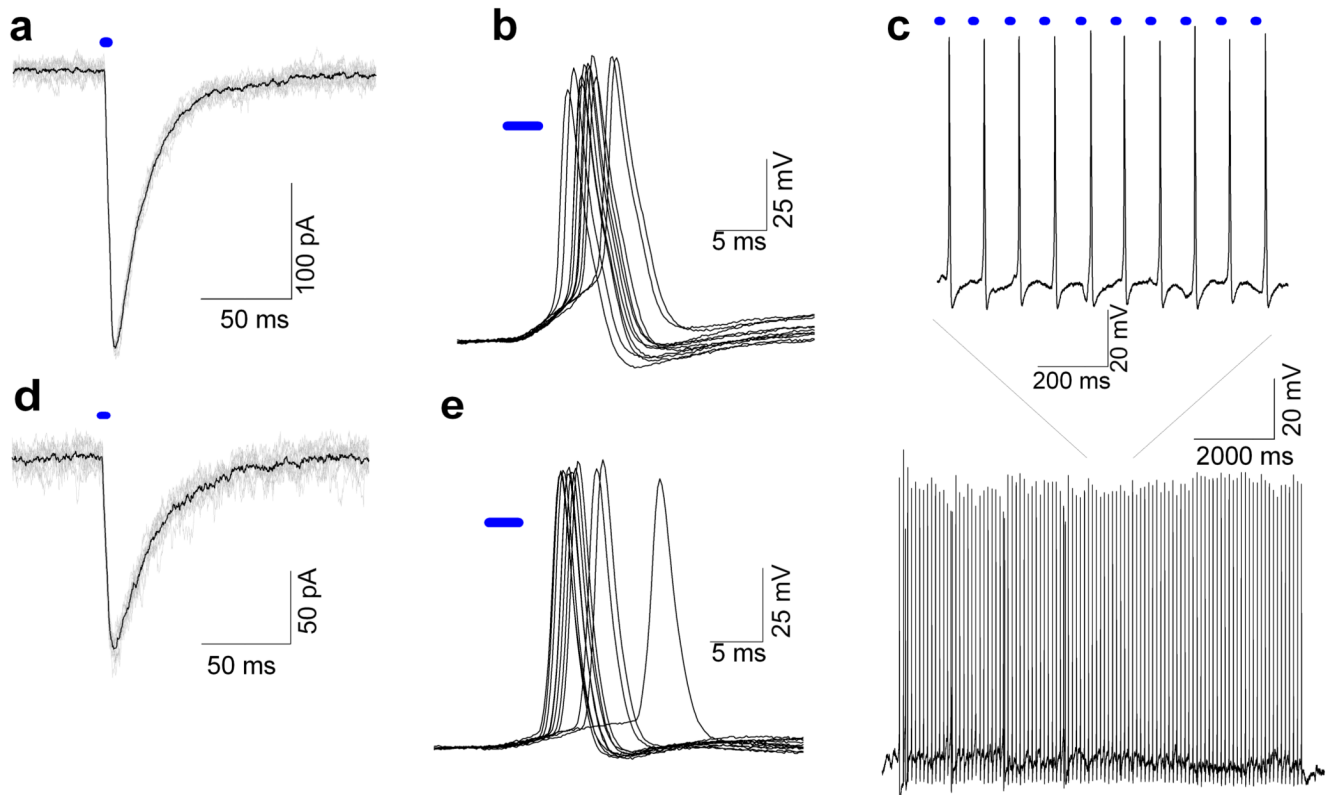
Fig. 2.
Optogenetic stimulation of PVN neurons expressing ChR2 25–30 days after injection of lentiviral vector OXY-ChR2-EYFP or AVP-ChR2-EYFP. (a) 10 consecutive (gray) and average (black) voltage-clamp traces (3 ms stimulation at 1 Hz) of OXY-ChR2-EYFP expressing neurons in the PVN recorded in the presence of AP5, CNQX and TTX. In this and all subsequent panels the blue bar represents the period of blue laser exposure. (b) Representative current-clamp traces of consecutive stimulations (3 ms, at 1 Hz) of OXY-ChR2-EYFP PVN neurons recorded in the presence of AP-5 and CNQX. (c) Reliable action potential firing during 10s stimulation at 10 Hz in OXY-ChR2-EYFP PVN neurons; detail shows 10 consecutive action potentials, (d) 10 consecutive (gray) and average (black) voltage-clamp traces (3 ms stimulation at 1 Hz) of AVP-ChR2-EYFP PVN neurons in the recorded in the presence of AP5, CNQX and TTX. (e) Representative current-clamp traces of consecutive stimulations (3 ms, at 1 Hz) of AVP-ChR2-EYFP PVN neurons recorded in the presence of AP-5 and CNQX. 12,
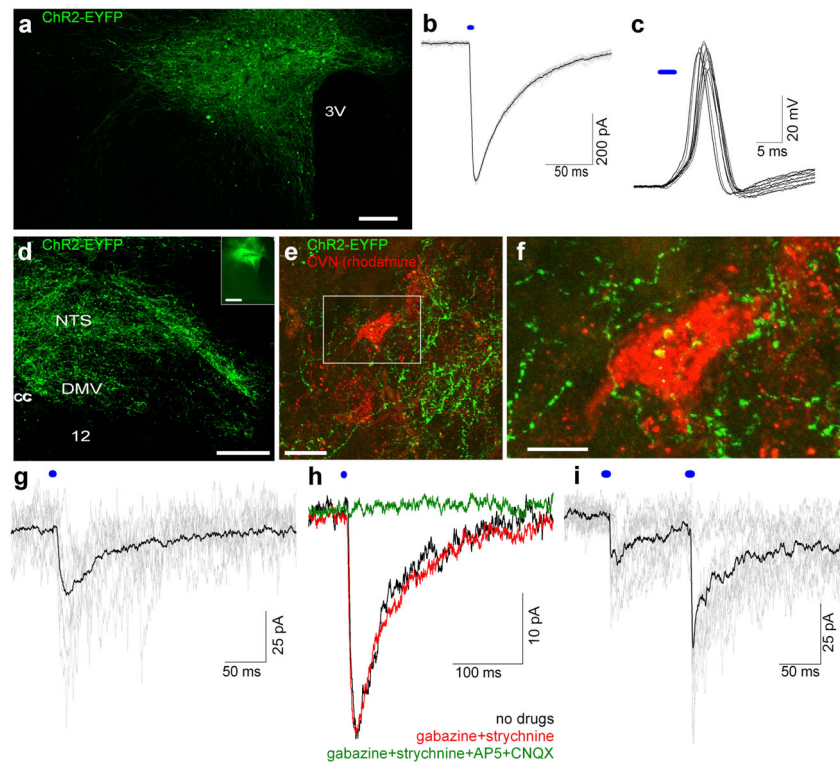
Fig. 3.
Lentiviral vector with strong neuronal promoter, Syn-ChR2-EYFP, expresses ChR2 in PVN neurons and optogenetic stimulation of long-range PVN projections in brain stem evokes EPSCs in CVNs (a) Syn-ChR2-EYFP expresses ChR2-EYFP in PVN neurons. Scale bar represents 50 µm. (b) 10 consecutive (gray) and average (black) voltage-clamp traces (3 ms stimulation at 1 Hz) of Syn-ChR2-EYFP expressing neurons in the PVN recorded in the presence of AP5, CNQX and TTX. (c) Representative current-clamp traces of 10 consecutive stimulations (3 ms, at 1 Hz) of Syn-ChR2-EYFP PVN neurons recorded in the presence of AP-5 and CNQX. (d) Dense network of distal axons of PVN neurons in brainstem dorsal vagal complex of Syn-ChR2-EYFP rat, 28 days after injection with inset of PVN injection site (scale bars represent 150 µm). (e) Cardiac vagal neurons (red) are surrounded by ChR2-EYFP PVN axons in the nucleus ambiguus (scale bar represents 25 µm). (f) Detail of (e) showing close apposition PVN axons to a CVN (scale represents 10 µm). (g) 7 consecutive (gray) and average (black) responses to 3 ms stimulation (at 2 Hz) of a CVN in the DMV. (h) Bath application of gabazine and strychnine reveals that response is an EPSC, which is completely blocked by AP-5 and CNQX (laser stimulation: 1ms at 2Hz). (i) 12 representative (gray) and average (black) responses to paired-pulse stimulation (3 ms at 10 Hz, 20s between sweeps) of a CVN in the DMV show paired-pulse facilitation. 12, Hypoglossal Nucleus; 3V, Third Ventricle; cc, Central Canal; DMV, Dorsal Motor Nucleus of the Vagus; NTS, Nucleus of the Solitary Tract.
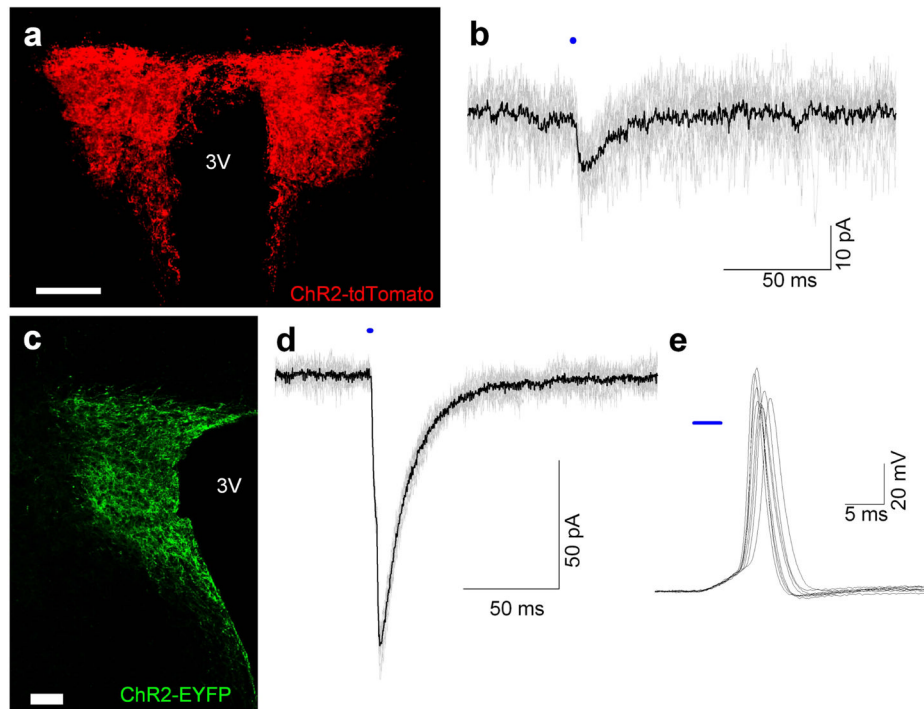
Fig. 4.
Sim1-Cre mice crossbred with ChR2 Cre-responder mice yields ChR2 expression in PVN
(a) Tile scan of the bilateral PVN of ChR2-tdTomato/Sim1 mouse at P35 (scale bar
represents 150 µm). (b) 10 consecutive (gray) and average (black) voltage-clamp traces (3
ms stimulation at 1 Hz) of PVN neuron of ChR2-tdTomato/Sim1 mouse. (c) PVN of P12
ChR2-EYFP/Sim1 mouse (scale bar represents 50 µm). (d) 10 consecutive (gray) and
average (black) voltage-clamp traces (3 ms stimulation at 1 Hz) of PVN neuron of ChR2-
EYFP/Sim1 mouse. (e) 8 consecutive action potentials of PVN neuron in ChR2-EYFP/Sim1
when stimulated briefly (3ms) at 0.05 Hz. 3V, Third Ventricle

Table 1

Lentiviral vectors used in this study

Lentiviral vector	Promoter to drive ChR2-EYFP expression	Titer [TU/ml]	Injection volume [nl]
Syn-ChR2-EYFP	Human synapsin I fragment	$2 - 7 \times 10^8$	50–200
AVP-ChR2-EYFP	Vasopressin	1×10^9	250–350
OXY-ChR2-EYFP	Oxytocin	2×10^8	250–350